

# SONAR SCENARIO A1: KILLER WHALE VS CHINOOK SALMON

MA Ainslie, TNO, Delft, Netherlands; and ISVR, University of Southampton, UK.  
M Zampolli, TNO, The Hague, Netherlands.

## 1 INTRODUCTION

The Validation of Sonar Performance Assessment Tools Symposium, organised by the Institute of Acoustics was held in Cambridge, UK on 7-9 April 2010. The meeting was held in memory of David E. Weston and consequently is also known as the "Weston Memorial Symposium". Two sonar scenarios were considered for the Weston Memorial Symposium, one man-made (low frequency active sonar) scenario and one bio-sonar scenario.

The bio-sonar scenario, inspired by the work of [Au et al 2004] on a **killer whale** (*Orcinus orca*) hunting its prey of **chinook salmon** (*Oncorhynchus tshawytscha*), is the subject of the present paper. The problem is specified in Sec. 2 and an example solution is presented in Sec. 3, including the effect of reverberation on detection performance (not part of the problem specified). Solutions for the orca-salmon problem specified in Sec. 2 are also given by [Ehrlich 2010].

## 2 PROBLEM SPECIFICATION

### 2.1 PROBLEM OVERVIEW

The problem is illustrated by Figure 1 below. Of practical interest is the question: At what distance  $R$  can the orca detect the fish by means of its active sonar against a background of wind noise? To eliminate the complications of an unknown detection threshold, the question posed for the Symposium scenario is instead: how does the signal to noise ratio vary with distance  $R$ ?

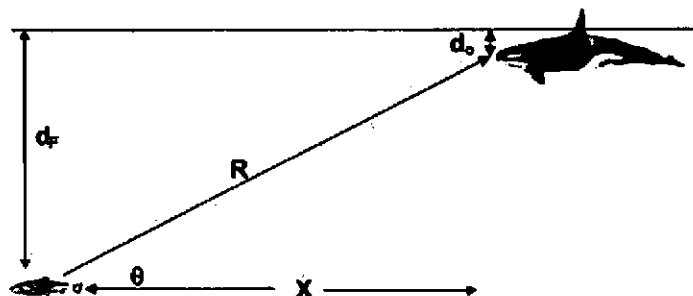


Figure 1: Illustration of orca v salmon geometry [reprinted from Au et al 2004]

Anticipated issues arising for this test case include:

How well can the broadband signal be represented by the propagation loss evaluated at a nominal centre frequency of 50 kHz?

For the purpose of calculating in-beam noise, can the array gain be approximated by the directivity index evaluated at the centre frequency?

## 2.2 Orca sonar properties

The orca's transmitted pulse has the following shape and spectrum (from Au et al Fig. 5):

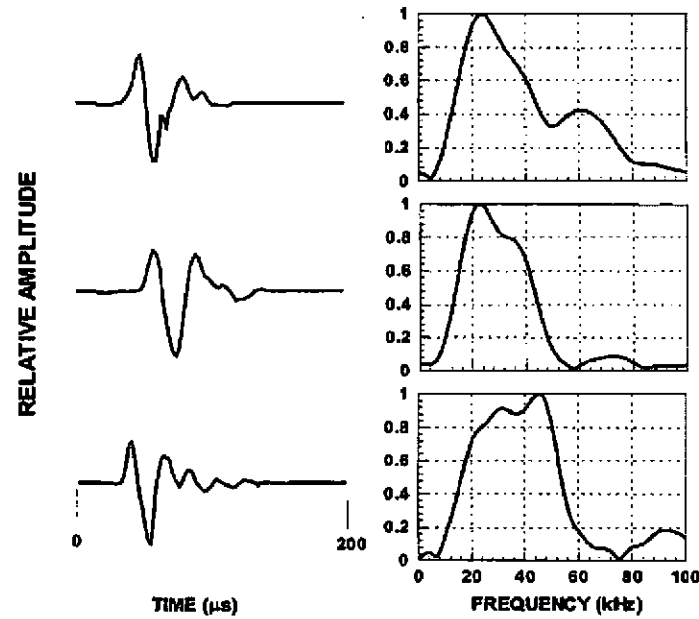


Figure 2: Example orca pulses and their spectra [reprinted from Au et al 2004]

For the Symposium scenario, the waveform is idealised using a Hann-shaded cosine pulse with an odd number of half cycles. The precise free-field pulse shape along the beam axis is

$$p_{Tx}(R, t)R = -Aw_{\text{Hann}}(t - R/c)\cos[2\pi f_0(t - R/c)], \quad (1)$$

where

$$w_{\text{Hann}}(t) = \begin{cases} 0 & t \leq -T/2 \\ \cos^2\left(\pi \frac{t}{T}\right) & -T/2 < t < T/2 \\ 0 & t \geq T/2 \end{cases} \quad (2)$$

and  $T$  is the pulse duration

$$T = \frac{2n+1}{2f_0} \quad (3)$$

with  $n = 2$ , corresponding to 5 half cycles.

The amplitude  $A$  is related to the peak to peak (p-p) source level approximately according to

$$SL_{pp} \approx 10 \log_{10} \frac{4A^2}{1 \mu\text{Pa}^2 \text{m}^2}. \quad (4)$$

The parameter  $A$  is the maximum amplitude of the product of distance with free field acoustic pressure (along the beam axis and in the far field of the source). Its value is chosen (see table below) to give a p-p source level close to 210 dB re  $1 \mu\text{Pa}^2 \text{m}^2$ , for consistency with Figure 3. The actual p-p source level is slightly less than the value given by Eq. (4). The pulse is completely described by Eq. (1), with the values of  $A$  and  $T$  from Table 1.

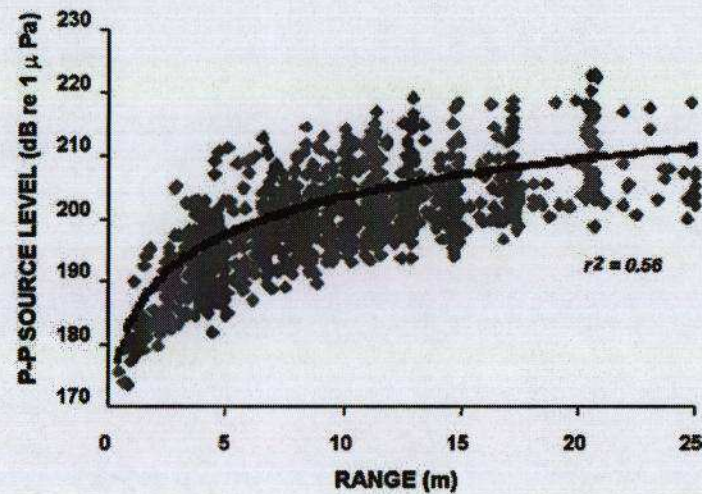


Figure 3: Measured p-p source levels vs orca-target separation [reprinted from Au et al 2004]

Following [Au et al 2004], a baffled circular transducer is assumed. The sonar properties are summarised in the following table:

parameter	symbol	value	notes
maximum amplitude	$A$	15 kPa m	See Eq. (1)
Centre frequency	$f_0$	50 kHz	From Au et al Fig 5
Duration	$T$	50 $\mu$ s	Hann-shaded pulse with odd number of half cycles. See Eq. (3)
Transducer diameter	$D$	10 cm	See Eq. (6)
Transducer depth	$d_0$	5 m	
Receiver bandwidth	$W$	60 kHz	pass band of 20-80 kHz
Receiver integration time	$t_{Rx}$	50 $\mu$ s	Assumed equal to the pulse duration

Table 1: Specification of orca sonar parameters

The beam pattern of an unshaded circular array is [Tucker & Gazey 1966, p180]

$$b(u) = [2J_1(u)/u]^2, \quad (5)$$

where  $J_1(u)$  is a first order Bessel function of the first kind. The argument  $u$  is a function of frequency  $f$ , diameter  $D$  and the angle  $\psi$  from the circle's axis of symmetry

$$u = (\pi D f / c) \sin \psi. \quad (6)$$

The half-power beam width (full width at half maximum) of an unshaded circular array is

$$\delta\theta_{\text{fwhm}} = 2 \arcsin\left(\frac{c}{\pi D f} u_0\right), \quad (7)$$

where  $u_0$  is the value of  $u$  for which  $b(u)$  is equal to  $\frac{1}{2}$

$$u_0 \approx 1.614. \quad (8)$$



For the Symposium scenario, the centre of the beam is assumed to point directly at the fish for both transmitter and receiver. The resulting beam pattern is a function of frequency and is plotted in Figure 4 for the frequencies 20, 50 and 80 kHz. The directivity index for an unbaffled array is

$$DI \approx 10 \log_{10} \left( 4\pi \frac{S}{\lambda^2} \right)$$

which at the centre frequency is about 20.4 dB.

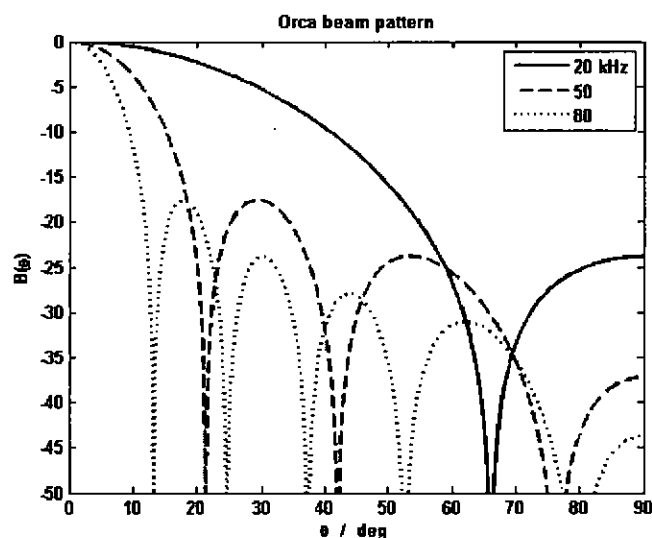


Figure 4: Orca beam pattern

## 2.3 Salmon properties

parameter	symbol	value
Fish depth	$d_F$	25 m
Fish length	$L$	80 cm
Target strength	TS	-30 dB re $m^2$

Table 2: Specification of salmon properties

The target strength can be estimated using the correlation equation from [Foote 1997]

$$TS - 10 \log_{10} \frac{L^2}{1 m^2} = -27.5 \text{ dB}, \quad (9)$$

which for  $L = 0.8$  m gives  $TS = -29.4$  dB re  $1 m^2$ , which is rounded to -30 dB for the test problem, as specified in Table 2.

## 2.4 Background parameters

The detection problem is assumed to be limited by wind noise (and not by reverberation nor by the orca's hearing threshold). The source level spectrum is given by the APL 1994 model [anon 1994] for unstable conditions (air cooler than water), i.e.,

$$\text{SDSL} = 41.2 + 22.4 \log_{10} V - 15.9 \log_{10} F - \log_{10} \delta \quad \text{dB re } \mu\text{Pa}^2 \text{ Hz}^{-1} \quad (10)$$

where  $F$  is the frequency in kHz

$$F \equiv \frac{f}{1 \text{ kHz}} \quad (11)$$

$V$  is the wind speed in m/s

$$V \equiv \frac{v}{1 \text{ m/s}} \quad (12)$$

and  $\delta=1$ .

Here SDSL is the dipole source level expressed as a spectral density per unit area of the sea surface. Using the noise model from [anon 1994], the noise spectral density level (NSDL) at depth  $z$  is then

$$\text{NSDL}(z) = \text{SDSL} + 10 \log_{10} [2\pi E_3(2\beta z)], \quad (13)$$

where  $\beta$  is the absorption coefficient (in nepers per unit distance) at the frequency of interest and  $E_3(x)$  is a third order exponential integral.

If there is no attenuation (i.e., if  $\beta z$  is small), the factor  $2E_3$  is equal to 1, so Eq. (13) would then simplify to

$$\text{NSDL} \approx \text{SDSL} + 10 \log_{10} \pi. \quad (14)$$

## 2.5 Environmental parameters

The water is assumed to have infinite depth, with a uniform sound speed. The attenuation coefficient is given by the following formula from [Jensen et al. 1994], converted to Np/m

$$\beta = \frac{\ln 10}{20000} \left( 3.3 \times 10^{-3} + \frac{0.11 F^2}{1 + F^2} + \frac{44 F^2}{4100 + F^2} + 3.0 \times 10^{-4} F^2 \right) \text{ Np/m} \quad (15)$$

parameter	symbol	value	notes
Wind speed	$v$	2 m/s	Measured at 10 m height.  Alternative wind speed value (optional) is 10 m/s.
Sound speed	$c$	1500 m/s	

Table 3: Specification of environment properties

## 2.6 Processing gain

The processing gain is that of the beamformer, i.e., the array gain. Array gain is defined as the gain in SNR from beamforming

$$AG \equiv \text{SNR}_{\text{out}} - \text{SNR}_{\text{in}} \quad (16)$$

where  $\text{SNR}_{\text{in}}$  is the signal to noise ratio at the input to the beamformer (i.e., in the water)

$$\text{SNR}_{\text{in}} = \text{EL}(R) - \text{NL} \quad (17)$$

and  $\text{SNR}_{\text{out}}$  is the signal to noise ratio at the beamformer output:

$$\text{SNR}_{\text{out}} = \text{IBSL}(R) - \text{IBNL}(R). \quad (18)$$

Here IBSL is the in-beam signal level and IBNL the in-beam noise level. To a first approximation IBSL can be replaced by the echo level (though an adjustment might be necessary due to the surface reflection entering through a sidelobe). The in-beam noise can be calculated using the model described on pp II-34 to II-40 of [anon 1994]. Using this model, the in-beam noise spectral density is (neglecting possible effects of near-surface bubbles)

$$N_f(R) = (10^{\text{SDSL}/10} \mu\text{Pa}^2/\text{Hz}) \int_{4\pi} b(u) \exp\left(-\frac{2\beta z}{\sin \theta_N}\right) \cos \theta_N d\theta_N d\phi, \quad (19)$$

In this equation  $\theta_N$  is the grazing angle,  $\phi$  is the azimuth angle of a ray path from a point on the sea surface to the orca,  $z$  is the depth at which the noise is evaluated, in this case the sonar depth  $d_0$ , and  $b(u)$  is the beam pattern given by Eq. (5). It is understood that the argument  $u$  is evaluated at the appropriate angle for the given geometry. The range dependence arises from the fact that the orca is assumed to direct the beam directly towards the fish, so the grazing angle of the centre of the beam increases as the animal homes in on its prey. Specifically, the grazing angle of the centre of the beam  $\theta_0$  is given by

$$\sin \theta_0(R) = \frac{d_F - d_0}{R}. \quad (20)$$

Integrating Eq. (19) over frequency and converting to decibels gives

$$\text{IBNL}(R) = 10 \log_{10} \left( \frac{\int N_f(R) df}{1 \mu\text{Pa}^2} \right). \quad (21)$$

The echo level (EL) is the maximum value of the sound pressure level (SPL) of the target echo averaged over the receiver integration time  $t_{\text{Rx}}$ , i.e.,

$$\text{EL}(R) = 10 \log_{10} \max \left[ \frac{1}{t_{\text{Rx}}} \int_{t_0 - t_{\text{Rx}}/2}^{t_0 + t_{\text{Rx}}/2} \frac{p_{\text{in}}^2(R, t)}{1 \mu\text{Pa}^2} dt \right], \quad (22)$$

where  $p_{\text{in}}(R, t)$  is the input to the beamformer, i.e., the acoustic pressure vs delay time  $t$  of the target echo at distance  $R$ , and the  $\max$  operation takes the maximum value of its argument as  $t_0$  is varied. The integration time  $t_{\text{Rx}}$  is specified in Table 1. Similarly, IBSL is the same function of the beamformer output:

$$\text{IBSL}(R) = 10 \log_{10} \max \left[ \frac{1}{t_{\text{Rx}}} \int_{t_0 - t_{\text{Rx}}/2}^{t_0 + t_{\text{Rx}}/2} \frac{p_{\text{out}}^2(R, t)}{1 \mu\text{Pa}^2} dt \right]. \quad (23)$$

The beamformer is understood to be normalised such that  $p_{in}$  and  $p_{out}$  are equal for the case of a plane wave signal, in which case EL and IBSL are also equal. If it is *assumed* that these two parameters are approximately equal, such that

$$IBSL(R) \approx EL(R), \quad (24)$$

it follows that

$$AG(R) \approx NL - IBNL(R). \quad (25)$$

## 2.7 Output formats

The main output is signal to noise ratio (SNR). The appropriate SNR depends on the assumed processing. For the Symposium problem the SNR is chosen to be that at the output of the beamformer, i.e.,

$$SNR(R) = IBSL(R) - IBNL(R). \quad (26)$$

Other outputs requested are:

Echo level vs slant range:  $EL(R)$

Noise SPL in pass band (independent of slant range): NL

$$NL = 10 \log_{10} \left( \frac{\int 10^{NSDL/10} df}{1 \text{ Hz}} \right), \quad (27)$$

Array gain vs slant range:  $AG(R)$ .

Participants in the Weston Memorial Symposium were encouraged to plot their output on a common format for ease of comparison, as follows.

SNR axis range: -10 to +40 dB

Echo level axis range: 50-100 dB re  $1 \mu\text{Pa}^2$

Array gain axis range: 5-30 dB

Distance (slant range  $R$ ) axis range: 0-500 m

### 3 EXAMPLE SOLUTION

#### 3.1 Broadband propagation loss

Neglecting the contribution from the surface reflected path, the narrow-band propagation factor is

$$F_{NB}(f, R, z_O, z_F) = \frac{\exp(-2\alpha(f)R)}{R^2}. \quad (28)$$

The corresponding narrow-band propagation loss, calculated as  $PL = -10\log_{10}(F_{in}/m^{-2})$ , is plotted in the upper graph of Figure 5. The broadband propagation factor is (using the shorthand  $f_{\pm} = f_0 \pm W/2$ )

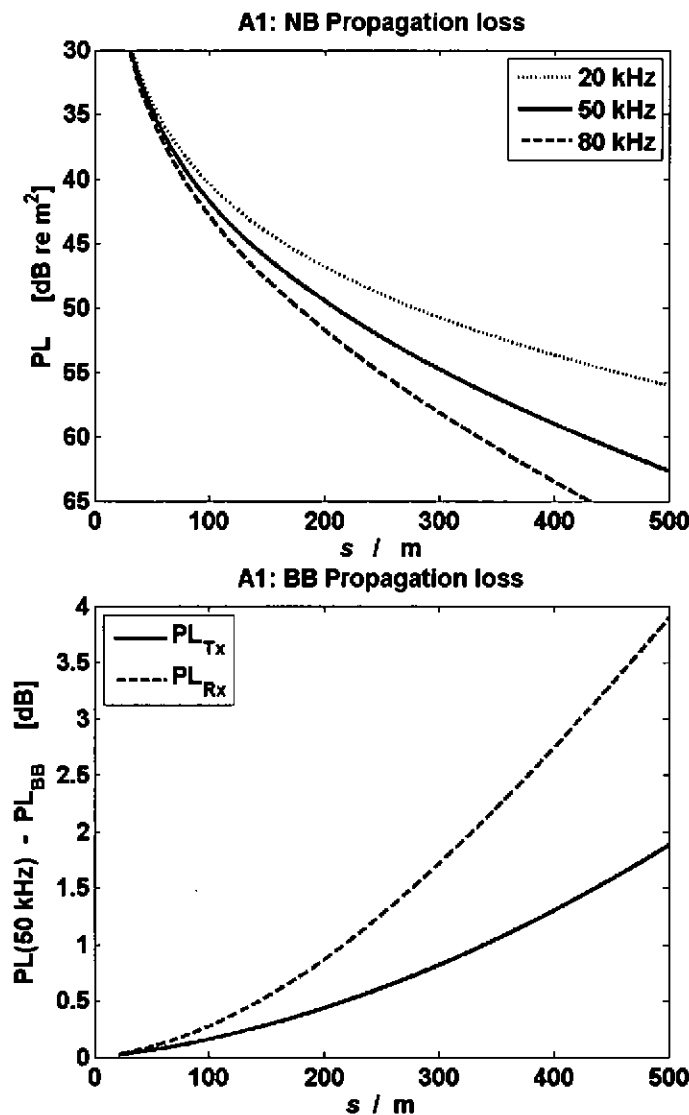


Figure 5: Upper: narrow-band PL vs range; lower: broadband correction relative to narrow-band PL at centre frequency [adapted from Ainslie 2010]



$$F_{BB} \approx \frac{1}{W} \int_{f_-}^{f_+} F_{NB}(f, R, z_O, z_F) df, \quad (29)$$

which for the one-way path from sonar transmitter to target, assuming a (locally) linear variation in the absorption coefficient with frequency

$$\alpha(f) \approx \alpha(f_0) + \frac{d\alpha}{df}(f - f_0) \quad (30)$$

is [Ainslie 2010]

$$F_{Tx} = \frac{1}{R^2} \exp(-2\alpha(f_0) R) \operatorname{sinhc}\left(\frac{d\alpha}{df} W R\right). \quad (31)$$

Similarly, the two-way propagation factor is

$$F_{Tx} F_{Rx} = \frac{1}{R^4} \exp(-4\alpha(f_0) R) \operatorname{sinhc}\left(2 \frac{d\alpha}{df} W R\right), \quad (32)$$

from which it follows that the propagation factor for the return path is

$$F_{Rx} = \frac{\exp(-2\alpha(f_0) R)}{R^2} \frac{\operatorname{sinhc}\left(2 \frac{d\alpha}{df} W R\right)}{\operatorname{sinhc}\left(\frac{d\alpha}{df} W R\right)}. \quad (33)$$

The broadband propagation loss (PL) is shown in the lower graph of Figure 5, in the form of a correction relative to the narrowband PL evaluated at the centre frequency. The physical reason why the PL is different (lower) for the return path is that the centre frequency, and hence the absorption coefficient is lower than for the outward path.

### 3.2 Noise-limited performance ( $v = 2$ to $10$ m/s)

Noise limited performance is considered for wind speeds 2, 6 and 10 m/s, with the simplifying assumption of an isotropic noise field.

#### 3.2.1 Broadband noise level and array gain

The broadband noise level is obtained by integrating the spectral density over the bandwidth  $f_-$  to  $f_+$ , and hence (neglecting absorption)

$$NL = 10 \log_{10} \left[ \frac{\pi}{0.59} \left( \left( \frac{1 \text{ kHz}}{f_-} \right)^{0.59} - \left( \frac{1 \text{ kHz}}{f_+} \right)^{0.59} \right) \right]. \quad (34)$$

The broadband array gain is then (assuming isotropic noise, for consistency)

$$AG = 10 \log_{10} \left( \frac{2.59 f_-^{-0.59} - f_+^{-0.59}}{0.59 f_-^{-2.59} - f_+^{-2.59}} \frac{\pi^2 D^2}{c^2} \right). \quad (35)$$

The result of this calculation is 16.5 dB. The effect of the (true) anisotropic noise field is considered by [Ehrlich 2010]).

### 3.2.2 Echo level and signal to noise ratio

The echo level EL and in-beam noise level (approximated as  $NL - AG$ ) are plotted vs target range in the upper graph of Figure 6, while the corresponding signal to noise ratio is shown in the lower graph. An arbitrary choice of a detection threshold of 10 dB would give detection ranges (not a required output) of 220 m, 120 m, 100 m for the three wind speeds considered. A summary of important parameters for this case is shown in Table 4.

parameter	symbol	value	
source level (RMS)	SL	198.2 dB	re $\mu\text{Pa}^2 \text{ m}^2$
target strength	TS	-30.0 dB	re $\text{m}^2$
noise level ( $v = 2$ m/s)	NL	75.0 dB	re $\mu\text{Pa}^2$
array gain	AG	16.5 dB	re 1

Table 4: Summary table: noise-limited performance

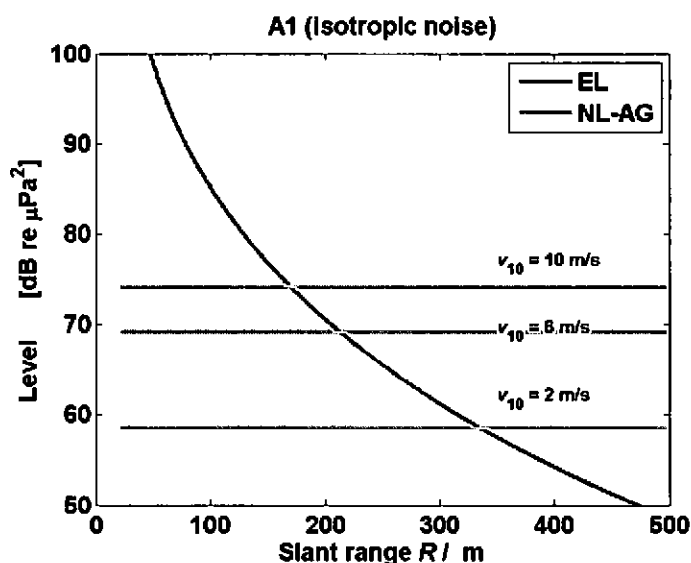
### 3.3 Effect of reverberation ( $v = 10$ m/s)

#### 3.3.1 Background level and array gain

The effect of introducing (surface) reverberation is to increase the background level and decrease the array gain at short ranges. The calculation assumes that the reverberation is dominated by scattering from wind-generated bubbles, and the surface scattering strength is calculated using the model of [anon 1994]. Noise and reverberation levels are shown in the upper graph of Figure 7, with the corresponding array gain in the lower graph. The assumption of isotropic noise is made as for the noise-limited situation, but reverberation is directional. Full details of the calculation method are described in Chapter 11 of [Ainslie 2010].

#### 3.3.2 Echo level and signal to background ratio

Echo and in-beam background levels are plotted vs target range in the upper graph of Figure 8, with the signal to background ratio (SBR) in the lower graph. It can be seen that the effect of reverberation is to reduce SBR in the range 60 to 150 m. In particular, the detection range of about 100 m for the noise-limited case (with the assumed DT = 10 dB) is reduced to 60 m in the presence of reverberation.





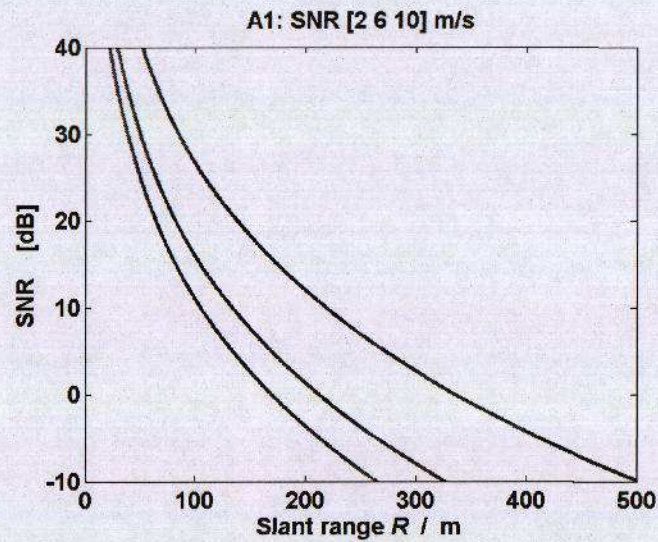


Figure 6: Upper: Echo level EL and in-beam noise level approximated as  $NL - AG$  vs target range for 2, 6 and 10 m/s; lower: signal to noise ratio for the same conditions [adapted from Ainslie 2010]

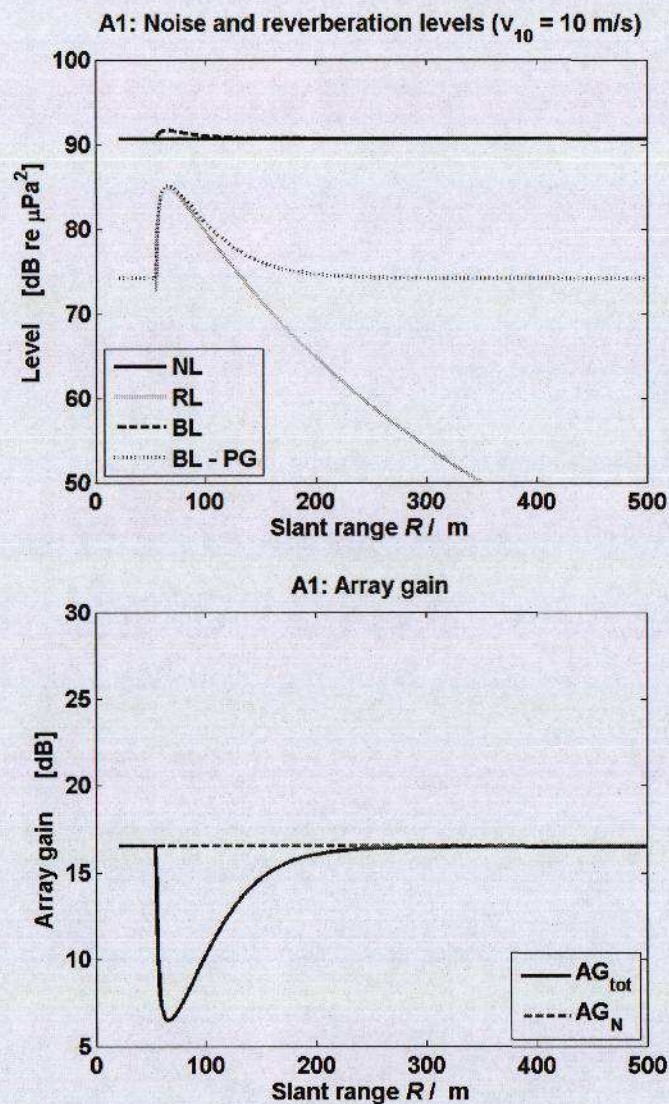


Figure 7: Upper: noise level, reverberation level, background level BL and in-beam background level approximated as  $BL - AG$  vs target range; lower: array gain vs target range [adapted from Ainslie 2010]

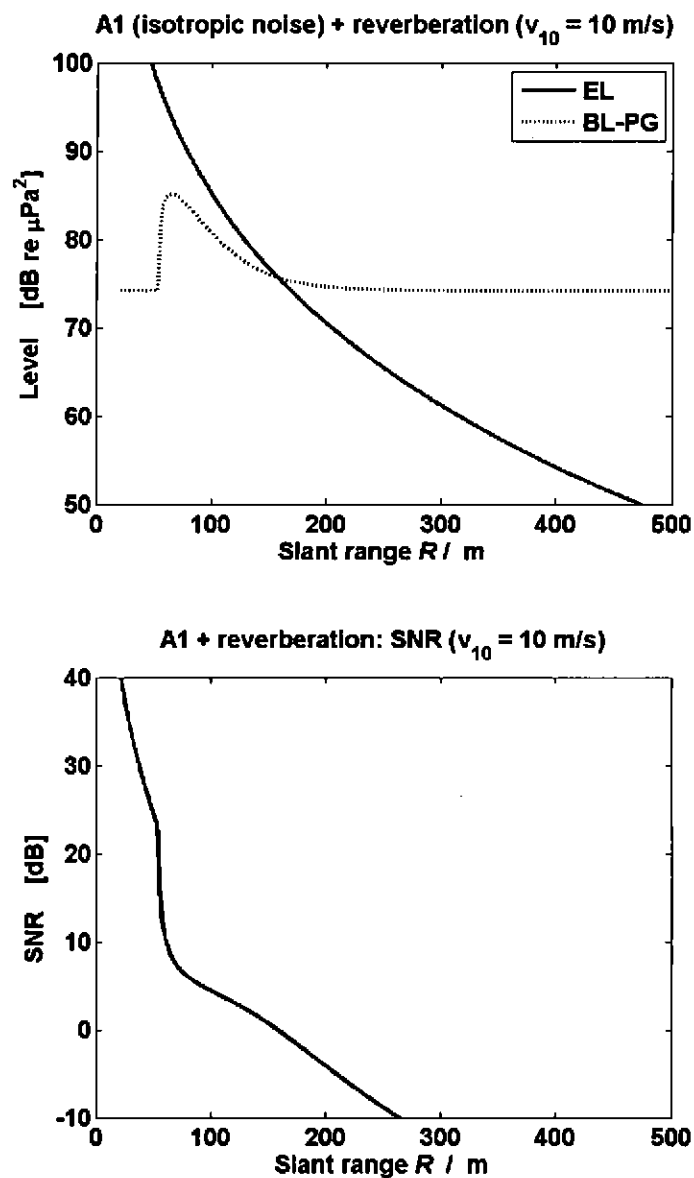


Figure 8: Upper: Echo level EL and the in-beam background level approximated as BL – AG vs target range for 10 m/s; lower: signal to background ratio for the same conditions [adapted from Ainslie 2010]



## 4 COMPARISON WITH EHRLICH [2010]

[Ehrlich 2010] presents results for echo level (EL), noise level (NL) and array gain (AG) for the problem specified in Sec. 2, and his results can be compared to those of Sec. 3 above. Differences between Ehrlich's results and the present paper are small (less than 2 dB) for two-way propagation loss (and hence also for EL) and for NL. Larger differences, of between 5 and 26 dB, are found in AG. These differences are attributed to the simplifying assumption made in the present paper (and not made by Ehrlich) that the noise field is isotropic.

Reverberation level is presented for different wind speeds, both in the present paper and [Ehrlich 2010]. These results are not included in the comparison because the reverberation is not part of the defined scenario for problem A1.

## 5 TARGET STRENGTH MODEL (SALMON)

The target strength of a salmon as a function of aspect and frequency can be estimated using a finite-element target scattering model. The acoustic frequencies of the source pulse range from 20 kHz to 80 kHz, and hence  $kL$ , with  $L = 80$  cm and  $k$  being the acoustic wave number in the water, ranges from 67 to 268. The impedance mismatch between the skin and flesh of the salmon and the water is relatively small, particularly when compared to the impedance mismatch of the swimbladder. Hence, the dominant contribution to the target strength can be expected to come from the swimbladder, which in this case is estimated to be about 10 cm long. The resulting  $kL$  for the swimbladder ranges thus from 8 to 34. This is well beyond the Rayleigh scattering regime for angles near broadside, which implies that the scattering response of the salmon can be expected to be angle dependent as one moves away from broadside insonification.

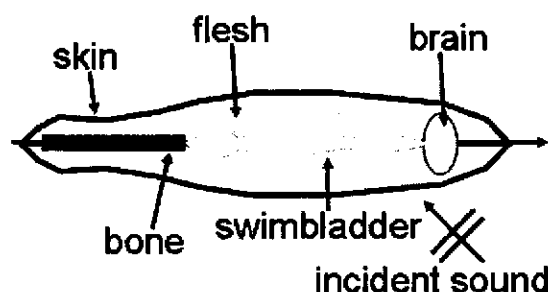


Figure 9: Schematic representation of an axisymmetric model, which can be used to estimate the target strength of a fish using a finite-element method.

The  $kL$  values encountered in this problem suggest that a fully three-dimensional model of the target scattering from the swimbladder alone is feasible on a standard desktop computer only for the lower frequencies, while for higher frequencies (up to 80 kHz) one would need to resort to a parallel solution. Also the computation of the target scattering for the entire fish is not feasible on a single desktop machine, given the high  $kL$  values of the problem. One possibility for obtaining efficiently an estimate of the scattering function of the salmon at the frequencies of interest here, is to model either the whole fish, including details such as skin, a backbone, a swimbladder, flesh and most relevant organs, or simply the swimbladder alone using an axisymmetric approximation for the geometry. An example of such an approximation, where the flesh, organs, skin and bones can be modelled as fluids or low shear-speed solids, including frequency dependent absorption, and the swimbladder can be modelled as a pressure release surface, is shown in Figure 9. This problem will be addressed in future work, using the modelling technique described in [Zampolli et al. 2007].

## 6 CONCLUSIONS AND WAY AHEAD

The broadband nature of the orca's sonar provides important corrections to both echo level (EL) and noise level (NL) terms in the sonar equation. These terms are well understood, as illustrated by the close agreement between the results of the present paper and those of [Ehrlich 2010]. Further, anisotropy of the ambient noise field has an important effect on the array gain (AG), resulting in differences of between 5 and 26 dB in this term. Future work is needed to confirm the magnitude of this effect, and to include reverberation in the problem specification.

## 7 REFERENCES

- [Ainslie 2010] M. A. Ainslie, Principles of Sonar Performance Modeling (Springer-Praxis, 2010, in press).
- [anon 1994] APL-UW High-Frequency Ocean Environmental Acoustic Models Handbook, APL-UW TR9407, AEAS 9501 October 1994, Applied Physics Laboratory, University of Washington, Seattle, Washington 98105-6698; available on-line from: - <http://staff.washington.edu/dushaw/epubs/APLTM9407.pdf>.
- [Au et al 2004] W. W. L. Au, J. K. B. Ford, J. K. Horne & K. A. Newman Allman, Echolocation signals of free-ranging killer whales (*Orcinus orca*) and modelling of foraging for chinook salmon (*Oncorhynchus tshawytscha*), J. Acoust. Soc. Am. 115, 901-909 (2004).
- [Ehrlich 2010] J. Ehrlich, Calculation with the models Mocassin and MSM for the test cases of the David Weston Memorial Symposium II, Proc. IOA Vol. 32, Part 2 (2010).
- [Foote 1997] K. G. Foote, Target strength of fish, in [M. J. Crocker (editor), Encyclopedia of Acoustics (Wiley, New York, 1997).] pp 493-500.
- [Haslett 1962] R. W. G. Haslett, Measurements of the dimensions of fish to facilitate calculations of echo-strength in acoustic fish detection, J. Conseil Perm Int. Explor. Mer 27, 261-269 (1962).
- [Jensen et al. 1994] F. B. Jensen, W. A. Kuperman, M. B. Porter & H. Schmidt, *Computational Ocean Acoustics* (AIP Press, New York, 1994).
- [Tucker & Gazey 1966] D. G. Tucker & B. K. Gazey, *Applied Underwater Acoustics* (Pergamon, Oxford, 1966).
- [Zampolli et al. 2007] M. Zampolli, A. Tesei, F.B. Jensen, N. Malm, J.B. Blottman, A computationally efficient finite element model with perfectly matched layers applied to scattering from axially symmetric objects, J. Acoust. Soc. Am. 122, pp. 1472 – 1485 (2007).